Environ. Sci. Technol. **2008,** *42,* 1787–1793

A Modified Parallel Artificial Membrane Permeability Assay for Evaluating the Bioconcentration of Highly Hydrophobic Chemicals in Fish

JUNG-HWAN KWON* AND
BEATE I. ESCHER

Department of Environmental Toxicology (Utox), Swiss Federal Institute of Aquatic Science and Technology (Eawag), Überlandstrasse 133, P.O. Box 611, 8600 Dübendorf, Switzerland

Received August 21, 2007. Revised manuscript received November 30, 2007. Accepted December 5, 2007.

Low cost in vitro tools are needed at the screening stage of assessment of bioaccumulation potential of new and existing chemicals because the number of chemical substances that needs to be tested highly exceeds the capacity of in vivo bioconcentration tests. Thus, the parallel artificial membrane permeability assay (PAMPA) system was modified to predict passive uptake/elimination rate in fish. To overcome the difficulties associated with low aqueous solubility and high membrane affinity of highly hydrophobic chemicals, we measured the rate of permeation from the donor poly(dimethylsiloxane) (PDMS) disk to the acceptor PDMS disk through aqueous and PDMS membrane boundary layers and term the modified PAMPA system "PDMS-PAMPA". Twenty chemicals were selected for validation of PDMS-PAMPA. The measured permeability is proportional to the passive elimination rate constant in fish and was used to predict the "minimum" in vivo elimination rate constant. The in vivo data were very close to predicted values except for a few polar chemicals and metabolically active chemicals, such as pyrene and benzo[a]pyrene. Thus, PDMS-PAMPA can be an appropriate in vitro system for nonmetabolizable chemicals. Combination with metabolic clearance rates using a battery of metabolic degradation assays would enhance the applicability for metabolizable chemicals.

Introduction

Bioaccumulation of hydrophobic organic chemicals has been of significant concern for decades (*1*–*3*). Bioaccumulation encompasses bioconcentration and biomagnification. Bioconcentration integrates the absorption, distribution, metabolism, and excretion of a chemical due to water-borne exposure, whereas biomagnification refers to ingestion of contaminated food (*3*). Diffusive and metabolic elimination rate constants are significant for assessing bioconcentration and biomagnification. Because of the difficulties associated with quantitatively assessing biomagnification potential, bioaccumulation assessment relies on the laboratory bioconcentration test, such as OECD 305E (*4*), which is cost-intensive and requires large numbers of laboratory animals.

* Corresponding author phone: +41 44 823 5567; fax: +41 44 823 5028; e-mail: Jung-Hwan.Kwon@eawag.ch.

However, the number of chemicals prioritized for bioaccumulation testing in different regulatory frameworks highly exceeds the laboratory capability. Driven by the United Nations Stockholm Convention in terms of Persistence, Bioaccumulation, Toxicity (PBT) criteria (*5*), for example, the new European chemical's legislation (REACH) requires a PBT assessment for all substances with yearly production volumes above 10 t (*6*). Therefore, low cost in vitro methods are required to replace in vivo tests in the screening stage.

Besides metabolism, passive absorption and elimination through surfaces (e.g., gills and skins) are some of the relevant processes that determine how much and how fast a chemical accumulates in the body (*7*). To evaluate bioconcentration rate parameters in fish, a parallel artificial membrane permeability assay (PAMPA), first introduced in pharmaceutical sciences to evaluate bioavailability of drugs (*8*–*10*), has been applied for the estimation of bioconcentration in fish (*11*). For highly hydrophobic chemicals, which are retained in the membrane due to their high sorption coefficients, permeability was measured in a cosolvent system such as 20% v/v acetonitrile in aqueous buffer (*12*), or elimination rates from lipid/dodecane membrane were measured (*11*). However, permeability obtained using a cosolvent system requires extrapolation, and direct elimination measurement requires a relatively large experimental setup and a long experimental time. Longer experimental time required for more hydrophobic chemicals renders the system susceptible to experimental artifacts, such as biodegradation and decrease of membrane stability.

To overcome the experimental limitations of classical PAMPA in case of hydrophobic chemicals, we modified a PAMPA system to directly measure the rate of permeation across membrane barriers using a thin (0.125 mm) poly(dimethylsiloxane) (PDMS) membrane as a membrane model. For highly hydrophobic chemicals, it is very difficult to evaluate how fast they cross the membrane by analyzing aqueous concentration due to their low aqueous solubility and high partition coefficient between membrane and water. Therefore, 1 mm thick PDMS disks were placed in the donor and the acceptor solution to serve as a passive dosing/sampling phase. Twenty organic chemicals, for which uptake and elimination rate constants were reported in literature for small fish, were chosen for validation of the modified PAMPA using PDMS (PDMS-PAMPA). The PDMS donor and the PDMS membrane were initially loaded with test chemicals. Concentrations in the three PDMS phases, the donor, the acceptor, and the membrane were measured after stirring to obtain apparent permeability. Apparent permeability values were then compared with in vivo elimination rate constants using a theoretical prediction model.

Theory and Design of the Modified PAMPA System

Diffusion Mass Transfer Model. In a simple two-compartment model, the rate of accumulation in fish is expressed according to eq 1,

$$\frac{dC_f}{dt} = k_a C_w - k_e C_f \quad (1)$$

where C_w and C_f are the concentrations of a chemical in water (mol cm^{-3}) and fish (mol g^{-1}), respectively, and k_a and k_e are first-order uptake and elimination rate constants in cm^{3}g^{-1}s^{-1} and s^{-1}, respectively. The rate constants, k_a and k_e are often described by a diffusion mass transfer model, which is the simplest bioconcentration model (*13*). According to this model, molecules pass through a series of biological

10.1021/es072088n CCC: $40.75
Published on Web 02/02/2008

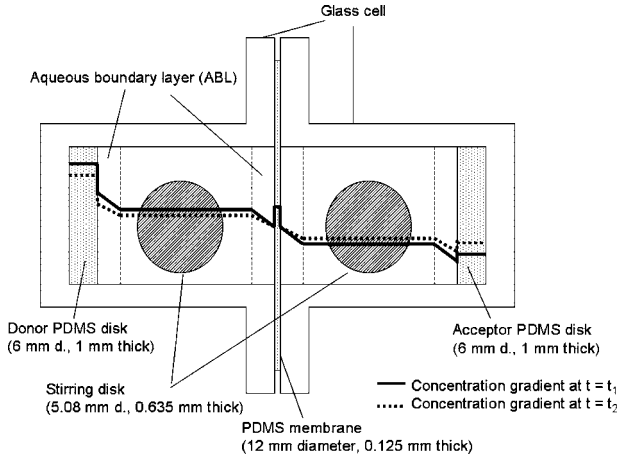

FIGURE 1. Cross-section of the PDMS PAMPA system. Solid and dashed line indicate concentration gradients at time = t_1 and t_2, respectively.

barriers composed of water and lipid bilayers and are stored in fatty tissues of the body (*14, 15*). Thus, mass transfer resistances in water and lipid membranes determine the passive uptake/elimination rate as shown in eqs 2 and 3 (*14, 15*),

$$k_a = P\frac{A}{W} = \frac{1}{\frac{\delta_w}{D_w} + \frac{\delta_m}{K_m D_m}}\frac{A}{W} \tag{2}$$

$$k_e = \frac{1}{\frac{\delta_w}{D_w} + \frac{\delta_m}{K_m D_m}}\frac{1}{(1-\alpha) + \alpha K_m}\frac{A}{W} = \frac{k_a}{(1-\alpha) + \alpha K_m} \tag{3}$$

where P is overall permeability through the biological barriers (cm s^{-1}), δ_w is the thickness of the aqueous boundary layer (ABL) (cm), D_w is aqueous diffusion coefficient ($cm^2 s^{-1}$), δ_m is the thickness of the membrane barrier (cm), D_m is membrane diffusion coefficient ($cm^2 s^{-1}$), α is the lipid content in the body, K_m is the lipid membrane-water partition coefficient ($cm^3 g^{-1}$), A is interface area (cm^2), and W is body weight (g).

As described in eqs 2 and 3, experimental k_a and k_e values depend on an allometric factor, the surface-to-weight ratio (A/W). It has been observed that rate constants decrease with increasing size (*16–18*). Thus, normalization of rate constants to a standard, for example, a fish of $W = 1$ g, is required to compare data from various literature sources. The surface-to-weight ratio decreases with increasing fish weight as described by the empirical formula derived by Sijm et al. (*17*) (eq 4).

$$\frac{A}{W} = (5.59 \pm 3.16) W^{-0.23 \pm 0.09} \tag{4}$$

Thus, literature values can be normalized to a standard 1 g fish by eq 5,

$$k_{a,norm}(\text{or } k_{e,norm}) = 0.23 k_a(\text{or } k_e) W \tag{5}$$

where $k_{a,\ norm}$ and $k_{e,\ norm}$ are normalized uptake and elimination rate constants for 1 g fish.

Design of the PDMS-PAMPA. A modified PAMPA (PDMS-PAMPA) system was developed to substantiate the conceptual diffusion mass transfer model described above. As shown in Figure 1, thick PDMS disks (6 mm diameter, 1 mm thick) were placed to serve as passive dosing/sampling phases. The two aqueous compartments adjacent to the dosing/sampling PDMS disks were separated by a thin PDMS membrane (12 mm diameter, 0.125 mm thick). The system of the PDMS membrane with the aqueous boundary layers at the interfaces can mimic biological barriers of mass transfer in fish. The thickness of aqueous boundary layer can be adjusted by stirring magnetic disks placed in the donor and the acceptor solution (*11, 19*) and will be identical adjacent to the PDMS disks and to the membrane.

According to a steady-state flux model, the changes in concentration of the acceptor and the donor PDMS with respect to time (t) are expressed by eq 6 when two PDMS disks are the same in size,

$$\frac{dC_A}{dt} = -\frac{dC_D}{dt} = \frac{P_{app}A}{V_{PDMS}}(C_D - C_A) \tag{6}$$

where C_A and C_D are concentrations in the acceptor and the donor (mol cm^{-3}), respectively, A is the interface area (cm^2), V_{PDMS} is the volume of the donor or the acceptor PDMS (cm^3), and P_{app} is the apparent permeability (cm s^{-1}). The P_{app} term describes all processes starting with desorption from the donor disk to uptake into the acceptor disk, thus a total of four ABLs with equal δ_w must be crossed. P_{app} is obtained by solving eq. 6, assuming negligible retention in the PDMS membrane and both the donor and the acceptor aqueous solution and an initial concentration of 0 in the acceptor disk.

$$P_{app} = -\frac{V_{PDMS}}{2At}\ln\left(1 - \frac{C_A}{C^*}\right) \tag{7}$$

C^* is the theoretical equilibrium concentration that represents the concentration in the donor and the acceptor PDMS after equilibrium is reached (C^* corresponds to $C_{D,t=0}/2$ without membrane retention). If membrane retention occurs, then there is a time lag (τ_{LAG}) between saturation of the membrane and permeation through the membrane (*20*). In this case, eq 8 may be used to calculate P_{app} using integration limits of eq 6 from τ_{LAG} to t, assuming that the membrane is first saturated with solute and permeation occurs after this saturation (*20*).

$$P_{app} = -\frac{V}{2A(t - \tau_{LAG})}\ln\left(1 - \frac{C_A}{C^*}\right) \tag{8}$$

The theoretical equilibrium concentration (C^*) in eq. 8 is less than that in eq 7 due to the sorption to the membrane. Time-course measurements are required to determine τ_{LAG}, C^*, and P_{app}. In addition, τ_{LAG} increases with increasing hydrophobicity, and the acceptor concentration (C_A) should be high enough to estimate all parameters. This makes assay time longer for more hydrophobic chemicals.

The driving force of mass transfer of hydrophobic organic pollutants is a concentration gradient in an ABL because the partition coefficient between PDMS and water (K_{PDMSw}) is high (*21*), and PDMS has a uniquely high permeability (*22–24*). Thus, it is reasonable to assume that the concentration gradient in the PDMS phase is negligibly small (shown as 0, Figure 1). In a symmetric system, such as the one depicted in Figure 1, the overall rate of solute transfer from the donor to the membrane should be equal to that from the membrane to the acceptor when the membrane concentration is the average of the donor and the acceptor, because concentration gradients on both sides are identical. As the solute permeates, the concentration gradient decreases. However, the membrane concentration should be invariant, indicating neither membrane retention nor accumulation. Therefore, one can use eq 7 for the calculation of P_{app}.

Using a steady diffusion theory, P_{app} is described by eq 9,

$$P_{app} = \frac{1}{\frac{\delta_{w,PAMPA}}{D_w} + \frac{\delta_{PDMS}}{D_{PDMS}K_{PDMSw}}}\frac{1}{K_{PDMSw}} \tag{9}$$

where $\delta_{w,PAMPA}$ is the overall thickness of the four ABLs (cm) in Figure 1, δ_{PDMS} is the thickness of the PDMS membrane (cm), D are diffusion coefficients in the ABL (subscript w) and PDMS (subscript PDMS) ($cm^2\ s^{-1}$), and K_{PDMSw} is the partition coefficient between PDMS and water. Thus, eq 9 is analogous to eq 3 if literature elimination rate constants are normalized (i.e., A/W is a constant). There are two requirements for the P_{app} values to be directly proportional to $k_{e,norm}$ (*1*): the ratio of aqueous resistance to the membrane resistance should be comparable between the in vitro and in vivo systems, and (*2*) K_{PDMSw} should be a good surrogate for K_m.

Experimental Section

Materials and Chemicals. Fifteen simple aromatic chemicals and five polyaromatic hydrocarbons (PAHs) were chosen for the evaluation of PDMS-PAMPA. Chemicals were of high purity and were purchased from Fluka (Buchs, Switzerland), Riedel-de-Haën (Seelze, Germany), and Sigma-Aldrich (St. Louis, Missouri). Medical grade poly(dimethylsiloxane) (PDMS) sheetings with a density of 1.17 g/cm^3 were purchased from Specialty Silicone Products, Inc. (Ballston Spa, New York). PDMS sheeting with 1 mm thickness was cut into 6 mm diameter disks for a passive dosing/sampling phase, and PDMS sheeting with 0.125 mm thickness was cut into 12 mm diameter disks to serve as membranes, as shown in Figure 1. Disks and membranes were cleaned in a Soxhlet extractor using *n*-hexane followed by methanol for 3 h each and were stored in methanol until use.

In Vivo Uptake/Elimination Rate Constants. In vivo uptake/elimination rate constants for the 20 selected chemicals were reported for small fish (0.1–10.0 g) by various authors (*15, 25–37*). Although rate constants were normalized based on their surface-to-weight ratio, the thicknesses of aqueous and membrane boundary layers (δ_w and δ_m) are thought to increase with increasing fish size (*15*). Thus, a narrow range of fish size was chosen for the evaluation of the physical model to avoid allometric effects other than A/W.

Measurement of Membrane Permeability. For hydrophobic chemicals with $K_{PDMSw} \geq 100$, a donor PDMS disk (6 mm diameter, 1 mm thick) was loaded with a mixture of 2−4 compounds by placing in a vial containing chemicals in a methanol/water (50/50, v/v) solution. Vials were shaken for 24 h to reach equilibrium between PDMS and the solution. The initial concentrations in the donor PDMS disk were between 7.8 and 84 $nmol/cm^3$. PDMS membranes (12 mm diameter, 0.125 mm thick) were loaded using the same procedure to make the initial chemical's concentration one half the concentration of the donor disk. For less hydrophobic chemicals with $K_{PDMSw} < 100$, donor PDMS disks were loaded using deionized water spiked with a chemical mixture. Aqueous retention is significant for them, and membrane retention is negligible. Thus, the aqueous solution after the equilibration with the donor PDMS disk was used as the donor solution to satisfy the assumptions underlying eq 7.

The "pre-loaded" donor PDMS and the "clean" acceptor PDMS were separated by the "pre-loaded" PDMS membrane and aqueous solution in the donor and the acceptor cell (approximately 0.16 cm^3 each), as described in Figure 1. A stainless steel magnetic disk (5.08 mm diameter, 0.635 mm thick, V&P Scientific, Inc., San Diego, California) was placed in the solution for stirring. After stirring for the indicated time at 300 rpm using a tumble stirrer (VP710, V&P Scientific, Inc.), both PDMS disks and membranes were taken and were extracted using acetonitrile or *n*-hexane for HPLC or GC analysis. Mass balance was mostly between 90 and 110%, indicating that system loss was negligible. Apparent membrane permeability (P_{app}) values were calculated using eq 7 for at least three stirring times using triplicate. All individual values were lumped to obtain mean P_{app}.

Instrumental Analyses. All chemicals, except for chlorinated benzenes, were analyzed by an HPLC system equipped with a Dionex P680 separation module and an ASI-100 automated sample injector (Dionex Softron GmbH, Germering, Germany). Elution solvents were water and acetonitrile at 1 mL/min. PAHs were separated on a C18 Supelcosil LC-PAH column (150 mm × 4.6 mm, 5 μm, Supelco, Bellefonte, Pennsylvania) at 40 °C and were detected using a RF-2000 fluorescence detector (Dionex) with an excitation wavelength (λ_{ex}) of 275 nm and an emission wavelength (λ_{em}) of 350 nm for naphthalene and phenanthrene, $\lambda_{ex} = 260$ nm and $\lambda_{em} = 420$ nm for anthracene and pyrene, and $\lambda_{ex} = 290$ nm and $\lambda_{em} = 430$ nm for benzo[*a*]pyrene. Phenol and anilines were separated on a Nucleodur C18 Gravity column (125 mm × 4 mm, 5 μm, Macherey-Nagel GmbH & Co., Oensingen, Switzerland) at ambient temperature and were detected using a UVD 340U diode array detector (Dionex) at their optimal absorption wavelengths.

For chlorinated benzenes, concentrations of *n*-hexane extracts were measured using a Fisons HRGC 8000 Series GC (Milan, Italy) equipped with a Fisons MD800 mass spectrometer. Chemicals were ionized by electron impact at 70 eV and were detected using selective ion monitoring. Ions were monitored at $m/z = 146$, 180, 216, 250, and 284 for di-, tri-, tetra-, penta-, and hexa-chlorinated benzenes, respectively. Extraction recoveries of all chlorinated benzenes were between 90 and 110%. Two microliters of *n*-hexane extract were injected in a split/splitless mode onto a DB-5MS column (15 m × 0.25 mm i.d., 0.25 μm film thickness, J&W Scientific, Folsom, California). Helium was a carrier gas at a constant pressure of 50 kPa. The injector and transfer line were maintained at 250 and 280 °C, respectively. Column temperature was held at 50 °C for 7.5 min, followed by a ramp of 5 °C/min to 150 °C without hold, followed by a ramp of 20 °C/min to 300 °C, and held for 2 min.

Results and Discussion

Evaluation of Literature In Vivo Data. The normalized uptake rate constants ($k_{a,norm}$) can be related to 1-octanol/water partition coefficients (K_{ow}), replacing K_m in eq 2 by K_{ow}. Nonlinear regression analysis using the literature $k_{a,norm}$ values in Table 1 yields eq 10 (see Supporting Information, Figure S1).

$$k_{a,norm} = K_{ow}/(21600 + 99.3K_{ow}) \quad (10)$$

According to this empirical relationship, $k_{a,norm}$ approaches 0.01 $cm^3g^{-1}s^{-1}$, lower than a typical respiratory ventilation volume of small fish (0.05 $cm^3g^{-1}s^{-1}$ for 60–100 mg guppy) (*38*), implying that diffusion through the ABL limits uptake/elimination. The corresponding ABL thickness is approximately 33 ± 20 μm if the diffusion coefficient of a typical chemical is assumed to be 6×10^{-6} cm^2/s (see Supporting Information, Section A, for derivation). Relatively large standard error of the estimation is due to the relative standard error associated with A/W (eq 4). The two mass transfer resistances (aqueous and membrane resistance) are equal when $\log K_{ow} = 2.34$. This is slightly lower than the commonly accepted breaking point of $\log K_{ow} \approx 3$ (*14, 15, 18, 39*). However, it should be noted that the correlation coefficient (r^2) was not very high and was strongly depended on in vivo data for more hydrophilic compounds. In particular, the two most hydrophilic chemicals chosen in this study, phenol and aniline, strongly influenced this value. In addition, the assumption in a diffusion model may not be valid for hydrophilic chemicals as they interact with polar head groups of lipid bilayers.

Median uptake rate constants for highly hydrophobic chemicals ($\log K_{ow} > 4$ and $\log K_{PDMSw} > 3$) are within 1 order of magnitude except for pyrene. Assuming that the uptake

TABLE 1. Octanol–water partition coefficients (log K_{ow}), PDMS–water partition coefficients (log K_{PDMSw}), aqueous diffusion coefficient (D_w), experimentally determined apparent permeability (P_{app}), median values of literature uptake ($k_{a,\ norm}$), and elimination rate constants ($k_{d,\ norm}$) for selected chemicals.

chemicals	CAS reg. No.	log K_{ow}[a]	log K_{PDMSw}[b]	D_w[c] $\times 10^{-6}$ cm²/s)	PDMS-PAMPA permeability P_{app} (cm/s)	median literature values[d] log $k_{a,norm}$ ($k_{a,norm}$ in $cm^3g^{-1}s^{-1}$)	median literature values[d] log $k_{e,norm}$ ($k_{e,norm}$ in s^{-1})	reference
phenol	108–95–2	1.50	−0.53	10.7	7.38 (±1.39) × 10^{-6}	−3.70	−4.95	*25*
aniline	62–53–3	0.90	0.01	10.8	1.49 (±0.15) × 10^{-5}	−2.64 (−2.65, −2.63)	−2.95 (−3.05, −2.87)	*26, 27*
2-chloroaniline	95–51–2	1.90	1.04	8.6	1.59 (±0.21) × 10^{-5}	−2.83	−4.01	*27*
3-chloroaniline	108–42–9	1.88	0.83	8.6	1.29 (±0.43) × 10^{-5}	−2.40	−3.45	*27*
2,4-dichloroaniline	554–00–7	2.78	1.69	7.3	9.27 (±1.53) × 10^{-6}	−2.52	−4.49	*27*
3,4-dichloroaniline	95–76–1	2.68	1.39	7.3	8.99 (±1.96) × 10^{-6}	−1.85 (−1.92, −1.79)	−3.36 (−3.48, −3.27)	*25, 27*
2,3,5,6-tetrachloroaniline	3481–20–7	4.10	3.25	5.7	4.45 (±1.35) × 10^{-7}	−1.94	−4.40	*28*
1,4-dichlorobenzene	106–46–7	3.45	2.91	7.8	1.18 (±0.41) × 10^{-6}	−2.41 (−3.00, −2.17)	−3.98 (−4.78, −3.71)	*29, 30*
1,2,3-trichlorobenzene	87–61–6	4.05	3.33	6.7	4.69 (±1.69) × 10^{-7}	−2.12 (−2.40, −1.88)	−5.58 (−5.73, −4.07)	*15, 29*
1,2,4-trichlorobenzene	120–82–1	4.02	3.33	6.7	3.61 (±1.25) × 10^{-7}	−1.98 (−2.32, −1.79)	−5.20 (−5.32, −5.10)	*30, 37*
1,3,5-trichlorobenzene	108–70–3	4.15	3.36	6.7	2.62 (±1.44) × 10^{-7}	−2.35	−4.11	*29*
1,2,3,5-tetrachlorobenzene	634–90–2	4.63	4.12	5.9	1.03 (±0.18) × 10^{-7}	−1.84 (−2.08, −1.81)	−5.26 (−5.47, −4.32)	*28, 31*
1,2,4,5-tetrachlorobenzene	95–94–3	4.63	4.03	5.9	1.17 (±0.21) × 10^{-7}	−1.56	−5.32	*30*
pentachlorobenzene	608–93–5	5.17	4.56	5.3	4.56 (±1.53) × 10^{-8}	−1.74 (−1.92, −1.43)	−5.50 (−6.50, −4.68)	*15, 29, 31*
hexachlorobenzene	118–74–1	5.31	4.91	4.9	1.35 (±0.51) × 10^{-8}	−1.45 (−2.26, −1.23)	−6.98 (−7.09, −6.23)	*15, 29*
naphthalene	91–20–3	3.35	2.75	8.6	1.36 (±0.21) × 10^{-6}	−1.88 (−2.01, −1.68)	−4.58 (−4.74, −4.50)	*32, 33*
anthracene	120–12–7	4.50	3.98	6.8	1.12 (±0.47) × 10^{-7}	−2.10 (−2.16, −1.65)	−5.69 (−6.12, −5.05)	*34–36*
phenanthrene	85–01–8	4.52	3.87	6.8	1.48 (±0.52) × 10^{-7}	−1.73 (−2.02, −1.60)	−4.94 (−5.85, −4.92)	*33, 35*
pyrene	129–00–0	5.00	4.36	6.2	4.73 (±1.88) × 10^{-8}	−2.74 (−2.79, −2.29)	−4.90 (−5.93, −4.77)	*33, 35*
benzo(a)pyrene	50–32–8	6.35	5.09	5.3	4.81 (±2.06) × 10^{-9}	−2.08 (−2.45, −1.97)	−5.66 (−6.01, −5.50)	*32, 34, 35*

[a] Values of log K_{ow} are recommended values in LOGKOW database (*45*). [b] Values are from ref *21*. Values from the shaking method are used when log $K_{PDMSw} \leq 3.5$. Values from the ABL permeation method are used when log $K_{PDMSw} > 3.5$. [c] Calculated using D_w (cm^2s^{-1}) = 2.7 × 10^{-4}/$MW^{0.71}$ (*46*). [d] Median values are used when multiple data are available for a chemical. Values in parentheses are the maximum and minimum literature values.

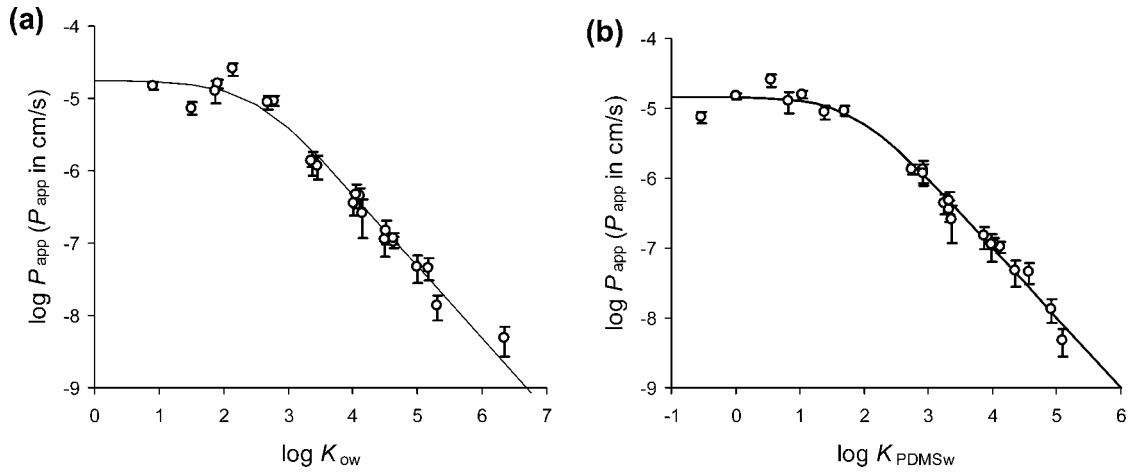

FIGURE 2. Relationships between experimental permeability (log P_{app}) and (a) log K_{ow} and (b) log K_{PDMSw}. Error bars denote standard deviations of measured permeability. Lines are fitted using eq 9. K_{ow} replaced K_{PDMSw} for panel a, assuming that K_{ow} is proportional to K_{PDMSw}.

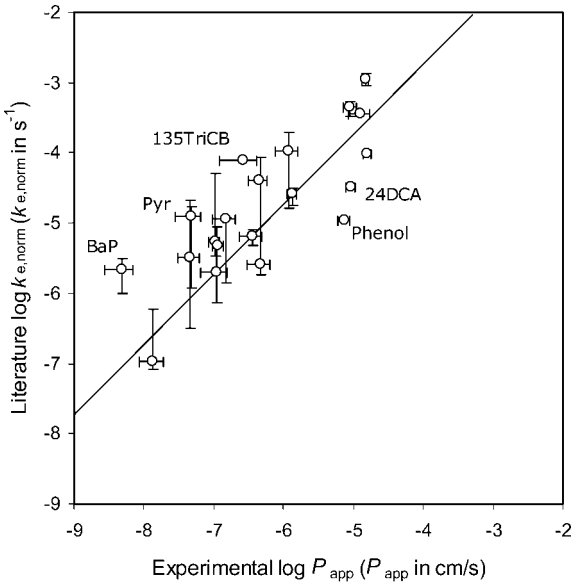

FIGURE 3. Relationship between normalized literature elimination rate constants (log $k_{e,norm}$) and PDMS-PAMPA permeability (log P_{app}). Line indicates the theoretical prediction model (eq 13). Vertical error bars denote the range of literature values when multiple values are available. Horizontal error bars denote standard deviations of measured permeability. Abbreviations: 24DCA, 2,4-dichloroaniline; 135TriCB, 1,3,5-trichlorobenzene; Pyr, pyrene; and BaP, benzo[a]pyrene.

of these hydrophobic chemicals is limited by aqueous diffusion, ABL thickness is estimated as $31 \pm 25\ \mu$m with $D_w = 6 \times 10^{-6}$ cm^{2}s^{-1} (eq 2). This is equivalent with that obtained by regression.

Membrane Permeability in the In Vitro PDMS-PAMPA System. The concentrations in the PDMS membrane did not change as compared to the initial concentration (see Supporting Information, Figure S2, with four PAHs as examples). The average $C_m/C_{m,t=0}$ values were mostly between 0.95 and 1.05, indicating that the fluxes coming into and going out of the membrane are identical, thus satisfying the assumption of steady-state flux. Therefore, the P_{app} can be easily determined even if the concentration in the acceptor disk is far below the equilibrium concentration.

All experimentally obtained apparent permeability values (P_{app}) are summarized in Table 1. Individual P_{app} values were not affected by stirring time (see Supporting Information, Figure S3), confirming that the experimental condition satisfies the steady-state diffusion during the experiment. Because the measured values were mostly stable within ± 0.2 log units, P_{app} could be measured within 24 h even for the most hydrophobic chemicals in this study.

As discussed above, P_{app} is analogous to the in vivo elimination rate constant and generally decreases with increasing hydrophobicity. Log P_{app} values are plotted against log K_{ow} (Figure 2a) and log K_{PDMSw} (Figure 2b). Log P_{app} does not change significantly in the lower log K_{ow} or log K_{PDMSw} ranges, but decreases with a negative unit slope as partition coefficients increase as expected from eq 9. Lines are fitted log P_{app} from log K_{ow} (as a surrogate for log K_{PDMSw}) or log K_{PDMSw} using eq 9, assuming that all chemicals have the same diffusivity. Mass transfer resistance in the ABL is equal to that in PDMS when log $K_{ow} = 2.44$ or log $K_{PDMSw} = 1.84$. This critical hydrophobicity value is close to the value obtained in the previous section and to the breaking point discussed in earlier work (*14, 15, 18, 39*). Thus, the PDMS-PAMPA at 300 rpm can be a good in vitro model because it satisfies the requirement that the overall diffusion is dominated by aqueous diffusion when the hydrophobicity of a chemical is greater than the critical value.

In Vitro to In Vivo Prediction Model. For highly hydrophobic chemicals, membrane diffusion is much faster than ABL diffusion both in vivo and in vitro. Thus, eqs 3 and 9 can be simplified by neglecting terms related with membrane diffusion:

$$k_{e,norm} = \frac{D_w}{\delta_{w,fish}} \frac{1}{\alpha K_m} \frac{A}{W} \quad (11)$$

$$P_{app} = \frac{D_w}{\delta_{w,PAMPA}} \frac{1}{K_{PDMSw}} \quad (12)$$

A simple relationship between in vivo log $k_{e,norm}$ and in vitro log P_{app} is then obtained by dividing eq 11 by eq 12 and taking the logarithm (eq 13).

$$\log k_{e,norm} = \log P_{app} + \log\left(\frac{\delta_{w,PAMPA}}{\delta_{w,fish}}\right) + \log\left(\frac{K_{PDMSw}}{\alpha K_m}\right) + \log\left(\frac{A}{W}\right) \quad (13)$$

There are three factors affecting the performance of the in vitro to in vivo prediction model, the ABL thickness, the partition coefficient to the membrane surrogate phase (PDMS in this study), and the surface-to-weight ratio of fish. The ABL thickness of the PAMPA system ($\delta_{w,PAMPA}$) can be obtained using the K_{PDMSw} values and the estimated D_w values of highly

hydrophobic chemicals (log K_{ow} > 4 and log K_{PDMSw} > 3) using eq 12. The $\delta_{w,PAMPA}$ term was estimated as 56 ± 15 μm (n = 12) and can, in the future, be adjusted by increasing stirring speed to mimic the in vivo situation at fish gills even more closely. The K_{PDMSw} is approximately 1 order of magnitude lower than K_{ow} by the empirical relationship shown in eq 14 (*21*).

$$\log K_{PDMSw} = 1.02 \log K_{ow} - 1.08 \quad (14)$$

Typical lipid contents of fish in the data set are 1.5–20%, with the approximate median value of 5% (*15, 28–31*). Assuming that K_{PDMSw} is also 1 order of magnitude lower than K_m, the $K_{PDMSw}/\alpha K_m$ term is approximately equal to 2. The surface-to-weight ratio of the standardized 1 g fish is 5.59 cm^2/g (eq 4). Thus, the intercept of eq 13 becomes 1.27. Figure 3 shows the relationship between normalized in vivo elimination rate constant (log $k_{e,norm}$) and apparent permeability (log P_{app}), with the line representing a theoretical prediction. Although there are uncertainties in the estimated intercept, most chemicals are close to the theoretical prediction within 0.5 log units, except for phenol, 2,4-dichloroaniline, 1,3,5-trichlorobenzene, pyrene, and benzo[a]pyrene.

The theoretical prediction model may not be applicable for rather hydrophilic compounds, because, as discussed above, underlying assumptions may not explain the permeation of those compounds. In vivo elimination rate constants, as well as uptake rate constants, for phenol and 2,4-dichloroaniline are much lower than for chemicals with a similar range of hydrophobicity (Table 1). Specific interaction such as hydrogen bonding may retard the rate of lipid membrane permeation for (bi)polar compounds. All other chemicals evaluated are on or slightly above the theoretically predicted line (Figure 3). This indicates that the model PAMPA system successfully estimates the rate of passive elimination that is the "minimal" rate of the elimination of chemicals in the body. The difference between in vivo data and theoretical prediction can be explained by metabolic degradation because the overall in vivo elimination rate constants are the sum of all relevant processes, including passive diffusion and metabolic degradation, the most significant processes among them (*3*). Pyrene and benzo[a]pyrene undergo phase I and phase II metabolic degradation in the liver of fish (*40–42*), and consequently, it comes as no surprise that their $k_{e,norm}$ values are more than 1 order of magnitude higher than the PDMS-PAMPA prediction. For example, Han et al. (*42*) estimated metabolic degradation rate constant for rainbow trout (*Oncorhynchus mykiss*) as 7.6×10^{-7} s^{-1}. This value is 1 order of magnitude higher than the predicted value (8.9×10^{-8} s^{-1}), indicating that the overall in vivo elimination rate for benzo[a]pyrene is dominated by metabolism.

To predict the whole body elimination rate and/or BCF/BAF, it is required to compare this predicted elimination rate with pseudofirst-order rate parameters in other processses. For example, growth rate may become significant for a highly hydrophobic chemicals (log K_{ow} > 6) that is resistant to metabolic degradation (*43*). Because passive elimination rate decreases with increasing thermodynamic partition coefficient between fish and water, there should be a critical passive elimination rate below the overall elimination dominated by growth.

A definitive advantage of the presented PDMS-PAMPA system lies in the fact that the prediction model to relate the in vitro results to in vivo is not just a best-fit model but is a theoretical model based on the underlying mechanistic processes. As such, it is generic and is not dependent upon the training set of chemicals, satisfying suggested criteria for the adequacy of the prediction models (*44*).

In conclusion, PDMS-PAMPA has a strong potential for the evaluation of passive elimination in the screening stage using a threshold level as B-criterion in PBT assessment. For example, chemicals with $P_{app} > 10^{-6}$ cm/s may be regarded as not bioaccumulative at the initial stage. This will reduce the number of chemical substances to be tested in the next step. Combination of PDMS-PAMPA with a battery of in vitro metabolism assays would enhance the applicability of the prediction for metabolizable chemicals. Furthermore, the predicted passive elimination rate constant as well as metabolic degradation rate constant can be used to estimate biomagnification/bioaccumulation because it is a result of the competition between food-bound uptake, fecal elimination, and growth.

Acknowledgments

We thank Dr. Alex Avdeef for valuable discussions and support by his team to get our PAMPA work started. We thank Thomas Wuethrich and Christoph Aeppli for their help with GC/MS analyses. We acknowledge 3R Research Foundation in Switzerland for funding (3R-Project 100-06).

Supporting Information Available

A relationship between log $k_{a,norm}$ and log K_{ow} (Figure S1) and C_m values and log P_{app} values with respect to stirring time (Figures S2 and S3). This material is available free of charge via the Internet at http://pubs.acs.org.

Literature Cited

(1) Weisbrod, A. V.; Burkhard, L. P.; Arnot, J.; Mekenyan, O.; Howard, P. H.; Russom, C.; Boethling, R.; Sakuratani, Y.; Traas, T.; Bridges, T.; Lutz, C.; Bonnell, M.; Woodburn, K.; Parkerton, T. Workgroup report: Review of fish bioaccumulation databases used to identify persistent, bioaccumulative, toxic substances. *Environ. Health Persp.* **2007**, *115*, 255–261.

(2) Mackay, D.; Fraser, A. Bioaccumulation of persistent organic chemicals: mechanisms and models. *Environ. Pollut.* **2000**, *110*, 375–391.

(3) Gobas, F. A. P. C.; Morrison, H. A., Bioconcentration and biomagnification in the aquatic environment. In *Handbook of Property Estimation Methods for Chemicals*, Boethling, R. S.; Mackay, D., Eds. CRC Press: Boca Raton, Florida, 2000.

(4) *Test Guideline 305. Bioaccumulation: Flow-through Fish Test*; Organization for Economic Co-Ordination and Development (OECD): 1996.

(5) *Stockholm Convention on Persistent Organic Pollutants (POPs)*; United Nations Environment Programme (UNEP): 2007.

(6) *EU, Regulation (EC) No. 1907/2006 of the European Parliament and of the Council of 18 December 2006 Concerning the Registration, Evaluation, Authorisation and Restriction of Chemicals;* Official Journal of the European Union, *L396/1*, **2006**.

(7) Randall, D. J.; Connell, D. W.; Yang, R.; Wu, S. S. Concentrations of persistent lipophilic compounds in fish are determined by exchange across the gills, not through the food chain. *Chemosphere* **1998**, *37*, 1263–1270.

(8) Kansy, M.; Senner, F.; Gubernator, K. Physicochemical high throughput screening: Parallel artificial membrane permeation assay in the description of passive absorption processes. *J. Med. Chem.* **1998**, *41*, 1007–1010.

(9) Wohnsland, F.; Faller, B. High-throughput permeability pH profile and high-throughput alkane/water log P with artificial membranes. *J. Med. Chem.* **2001**, *44*, 923–930.

(10) Avdeef, A.; Strafford, M.; Block, E.; Balogh, M. P.; Chambliss, W.; Khan, I. Drug absorption in vitro model: filter-immobilized artificial membranes 2. Studies of the permeability properties of lactones in Piper methysticum Forst. *Eur. J. Pharm. Sci.* **2001**, *14*, 271–280.

(11) Kwon, J. H.; Katz, L. E.; Liljestrand, H. M. Use of a parallel artificial membrane system to evaluate passive absorption and elimination in small fish. *Environ. Toxicol. Chem.* **2006**, *25*, 3083–3092.

(12) Ruell, J. A.; Tsinman, O.; Avdeef, A. Acid−base cosolvent method for determining aqueous permeability of amiodarone, itraconazole, tamoxifen, terfenadine and other very insoluble molecules. *Chem. Pharm. Bull.* **2004**, *52*, 561–565.

(13) Barber, M. C. A review and comparison of models for predicting dynamic chemical bioconcentration in fish. *Environ. Toxicol. Chem.* **2003**, *22*, 1963–1992.

(14) Gobas, F. A. P. C.; Opperhuizen, A.; Hutzinger, O. Bioconcentration of hydrophobic chemicals in fish — relationship with membrane permeation. *Environ. Toxicol. Chem.* **1986**, *5*, 637–646.
(15) Sijm, D. T. H. M.; van der Linde, A. Size-dependent bioconcentration kinetics of hydrophobic organic-chemicals in fish based on diffusive mass-transfer and allometric relationships. *Environ. Sci. Technol.* **1995**, *29*, 2769–2777.
(16) Gobas, F. A. P. C.; Mackay, D. Dynamics of hydrophobic organic-chemical bioconcentration in fish. *Environ. Toxicol. Chem.* **1987**, *6*, 495–504.
(17) Sijm, D. T. H. M.; Verberne, M. E.; de Jonge, W. J.; Pärt, P.; Opperhuizen, A. Allometry in the uptake of hydrophobic chemicals determined in-vivo and in isolated-perfused gills. *Toxicol. Appl. Pharmacol.* **1995**, *131*, 130–135.
(18) Hendriks, A. J.; van der Linde, A.; Cornelissen, G.; Sijm, D. T. H. M. The power of size. 1. Rate constants and equilibrium ratios for accumulation of organic substances related to octanol-water partition ratio and species weight. *Environ. Toxicol. Chem.* **2001**, *20*, 1399–1420.
(19) Avdeef, A.; Nielsen, P. E.; Tsinman, O. PAMPA — a drug absorption in vitro model 11. Matching the in vivo unstirred water layer thickness by individual-well stirring in microtitre plates. *Eur. J. Pharm. Sci.* **2004**, *22*, 365–374.
(20) Avdeef, A., *Absorption and Drug Development: Solubility, Permeability, and Charge State*; John Wiley & Sons, Inc.: New York, 2003.
(21) Kwon, J. H.; Wuethrich, T.; Mayer, P.; Escher, B. I. Dynamic permeation method to determine partition coefficients of highly hydrophobic chemicals between poly(dimethylsiloxane) and water. *Anal. Chem.* **2007**, *79*, 6816–6822.
(22) Rusina, T. P.; Smedes, F.; Klanova, J.; Booij, K.; Holoubek, I. Polymer selection for passive sampling: A comparison of critical properties. *Chemosphere* **2007**, *68*, 1344–1351.
(23) Ai, J. Solid phase microextraction for quantitative analysis in nonequilibrium situations. *Anal. Chem.* **1997**, *69*, 1230–1236.
(24) Mayer, P.; Vaes, W. H. J.; Hermens, J. L. M. Absorption of hydrophobic compounds into the poly(dimethylsiloxane) coating of solid-phase microextraction fibers: High partition coefficients and fluorescence microscopy images. *Anal. Chem.* **2000**, *72*, 459–464.
(25) Ensenbach, U.; Nagel, R. Toxicokinetics of xenobiotics in zebrafish — comparison between tap and river water. *Comp. Biochem. Phys. C* **1991**, *100*, 49–53.
(26) Bradbury, S. P.; Dady, J. M.; Fitzsimmons, P. N.; Voit, M. M.; Hammermeister, D. E.; Erickson, R. J. Toxicokinetics and metabolism of aniline and 4-chloroaniline in medaka (*Oryzias-Latipes*). *Toxicol. Appl. Pharmacol.* **1993**, *118*, 205–214.
(27) Kalsch, W.; Nagel, R.; Urich, K. Uptake, elimination, and bioconcentration of 10 anilines in zebrafish (Brachydanio Rerio). *Chemosphere* **1991**, *22*, 351–363.
(28) Dewolf, W.; Yedema, E. S. E.; Seinen, W.; Hermens, J. L. M. Bioconcentration kinetics of chlorinated anilines in guppy *Poecilia Reticulata*. *Chemosphere* **1994**, *28*, 159–167.
(29) Könemann, H.; Vanleeuwen, K. Toxico-kinetics in fish — accumulation and elimination of 6 chlorobenzenes by guppies. *Chemosphere* **1980**, *9*, 3–19.
(30) Smith, A. D.; Bharath, A.; Mallard, C.; Orr, D.; Mccarty, L. S.; Ozburn, G. W. Bioconcentration kinetics of some chlorinated benzenes and chlorinated phenols in American flagfish, *Jordanella Floridae* (Goode and Bean). *Chemosphere* **1990**, *20*, 379–386.
(31) Banerjee, S.; Sugatt, R. H.; Ogrady, D. P. A simple method for determining bioconcentration parameters of hydrophobic compounds. *Environ. Sci. Technol.* **1984**, *18*, 79–81.
(32) McCarthy, J. F.; Jimenez, B. D. Reduction in bioavailability to bluegills of polycyclic aromatic-hydrocarbons bound to dissolved humic material. *Environ. Toxicol. Chem.* **1985**, *4*, 511–521.
(33) Jonsson, G.; Bechmann, R. K.; Bamber, S. D.; Baussant, T. Bioconcentration, biotransformation, and elimination of polycyclic aromatic hydrocarbons in sheepshead minnows (*Cyprinodon variegates*) exposed to contaminated seawater. *Environ. Toxicol. Chem.* **2004**, *23*, 1538–1548.
(34) Spacie, A.; Landrum, P. F.; Leversee, G. J. Uptake, depuration, and biotransformation of anthracene and benzo[a]pyrene in bluegill sunfish. *Ecotox. Environ. Safety* **1983**, *7*, 330–341.
(35) Djomo, J. E.; Garrigues, P.; Narbonne, J. F. Uptake and depuration of polycyclic aromatic hydrocarbons from sediment by the zebrafish (*Brachydanio rerio*). *Environ. Toxicol. Chem.* **1996**, *15*, 1177–1181.
(36) Linder, G.; Bergman, H. L.; Meyer, J. S. Anthracene bioconcentration in rainbow-trout during single-compound and complex-mixture exposures. *Environ. Toxicol. Chem.* **1985**, *4*, 549–558.
(37) van Eck, J. M. C.; Koelmans, A. A.; Deneer, J. W. Uptake and elimination of 1,2,4-trichlorobenzene in the guppy (*Poecilia reticulate*) at sublethal and lethal aqueous concentrations. *Chemosphere* **1997**, *34*, 2259–2270.
(38) Erickson, R. J.; Mckim, J. M. A model for exchange of organic-chemicals at fish gills — flow and diffusion limitations. *Aquat. Toxicol.* **1990**, *18*, 175–197.
(39) Hawker, D. W.; Connell, D. W. Influence of partition-coefficient of lipophilic compounds on bioconcentration kinetics with fish. *Wat. Res.* **1988**, *22*, 701–707.
(40) Livingstone, D. R. The fate of organic xenobiotics in aquatic ecosystems: quantitative and qualitative differences in biotransformation by invertebrates and fish. *Comp. Biochem. Phys. A* **1998**, *120*, 43–49.
(41) Luthe, G.; Stroomberg, G. J.; Ariese, F.; Brinkman, U. A. T.; van Straalen, N. M. Metabolism of 1-fluoropyrene and pyrene in marine flatfish and terrestrial isopods. *Environ. Toxicol. Pharm.* **2002**, *12*, 221–229.
(42) Han, X.; Nabb, D. L.; Mingoia, R. T.; Yang, C. H. Determination of xenobiotic intrinsic clearance in freshly isolated hepatocytes from rainbow trout (*Oncorhynchus mykiss*) and rat and its application in bioaccumulation assessment. *Environ. Sci. Technol.* **2007**, *41*, 3269–3276.
(43) Nichols, J. W.; Fitzsimmons, P. N.; Burkhard, L. P. In vitro−in vivo extrapolation of quantitative hepatic biotransformation data for fish. II. Modeled effects on chemical bioaccumulation. *Environ. Toxicol. Chem.* **2007**, *26*, 1304–1319.
(44) Worth, A. P.; Balls, M. The principles of validation and the ECVAM validation process. *ATLA, Altern. Lab. Anim.* **2004**, *32*, 623–629.
(45) Sangster Research Laboratory. LOGKOW — A databank of evaluated octanol−water partition coefficient (log P). http://logkow.cisti.nrc.ca/logkow/index.jsp. (Accessed Nov. 30, 2007).
(46) Schwarzenbach, R. P.; Gschwend, P. M.; Imboden, D. M., *Environmental Organic Chemistry,* 2nd ed.; Wiley: New York, 2003.

ES072088N